# De-Novo Structural Elucidation of Acylglycerols by Collision-induced dissociation of odd-Electron Ion Precursors and by Electron Activated Dissociation of even-Electron Ion Precursors

Patrick Mueller and Gérard Hopfgartner*

Life Sciences Mass Spectrometry, Department of Inorganic and Analytical Chemistry, University of Geneva, 24 Quai Ernest Ansermet, CH-1211 Geneva 4, Switzerland

*corresponding author at e-mail:gerard.hopfgartner@unige.ch

Orcid: Patrick Mueller 0000-0003-1597-0299

Orcid: Gérard Hopfgartner 0000-0002-9087-606X

Short Title: Structural elucidation of acylglycerols using odd-electron precursor CID

Keywords: SFC-MS, atmospheric pressure photoionization, radical cation, collision induced dissociation, electron activated dissociation, acylglycerols

## ABSTRACT

State-of-the art mass-spectrometry can resolve double bond positions, fatty acid attachments and *sn*-positions of lipids but often lacks sensitivity, requires long reaction times and dedicated instrumentation. Atmospheric pressure photoionization using chlorobenzene as dopant (dAPPI) showed to form odd electron (OE) ion precursors generating rich spectra by collision induced dissociation (CID). In this study 33 model acylglycerols were analyzed using dAPPI-CID for sn-position and double bond (DB) assignment. Acylglycerols with ≤ 3 DB formed OE ions $[M-H]^+$ and those ≥ 4 DB $M^{+\bullet}$ ions. OE-CID acylglycerol precursors generated characteristic fragments intensity ratios for *sn*-positions and several DB fragment series. Compared to electron-activated dissociation (EAD) of even electron precursors formed by ESI, OE-CID showed better fragments intensities with shorter MS cycle times. For OE-CID de-novo DB assignments was performed by following loss series, such as $M\text{-}CH_3(CH_2)_n$, with intensity maxima at the beginning of DB positions. For each DB lost, a Δ2H shift is observed ($M\text{-}CH_3(CH_2)_n$ $\Delta 2H_x$) and used for the annotation of following DB. Additional loss series were observed after fatty acid loss ($(M\text{-}FA\text{-}3H\text{-}CH_3(CH_2)_n$), which showed *sn*-position related intensity alterations. This allowed to assign DB to specific fatty acids and evaluate the stoichiometry of DB positions. MsRadaR, a R package with a de-novo structural elucidation pipeline was developed for data visualization and to assign DB position, applicable for both EAD and OE-CID. Supercritical fluid chromatography coupled to dAPPI/CID was applied for the analysis of linseed oil where 36 acylglycerols were detected as radical cation. Furthermore, the approach was applied for the characterization by SFC-APPI-CID of fatty acids and cholesteryl esters using SWATH analysis of standards and data dependent acquisition of plasma samples using selected monitoring mode as survey scan and enhanced product ion as dependent scan.

## INTRODUCTION

Acylglycerols are lipid molecules, composed of a glycerol moiety, esterified with one (monoglycerides) to three fatty acids (triglycerides) [1]. Triglycerides play a crucial role as the main storage form of fatty acids for energy homeostasis and lipid transport in Eukarya, where on demand enzymatic hydrolysis can release fatty acids as well as di-and monoglycerides. This does entail triglycerides in the metabolism of mono-and diglycerides, which are involved in various cellular signaling pathways and act as precursors for other lipid molecules, such as phospholipids and bioactive fatty acids[2, 3]. Certainly, the vast involvement in metabolic processes allows to utilize acylglycerols as biomarkers for abnormal phenotypes caused by disease, medication and drug abuse, including metabolic storage disorders, radiation-induced fibrosis and tetrahydrocannabinol consumption[3-5]. Despite that, differences in the triglyceride compositions of vegetable oils can be used to detect food fraud, whereas acylglycerols and their degradation products are used to probe the composition and age of artworks, archaeological objects and fingerprints [6-9]. Last, acylglycerols and other glycerolipids are increasingly used for pharmaceutical products as active substance and excipients, such as lipid nanoparticles for mRNA vaccines. [10-12].

Over the years, mass spectrometry (MS) has established as standard tool for glycerolipid analysis, where soft ionization techniques, such as electrospray ionization (ESI), atmospheric-pressure chemical ionization (APCI) or atmospheric-pressure photoionization (APPI) with high-resolution mass spectrometry (HRMS) and collision-induced dissociation of even electron precursors (EE-CID) enable identification glycerolipid species and their fatty acid composition [13, 14]. In the case of ammonium adducts of triglycerides, CID fragmentation allows to assign stereospecific numbering(*sn*) positions of fatty acids at the glycerol backbone based on intensity ratios of fatty acid losses, with a preference for *sn*-1/3 losses.

In order to understand the biological significance of single glycerolipids in complex systems more reliable and advanced MS techniques are necessary to distinguish between structural isomers, which differ in *sn*-positions, carbon branching sites within fatty acids as well as double bond localizations and their corresponding stereo configuration [15]. Various de-novo structural analysis approaches were reported to spot double bond positions, including Ozon-induced dissociation (OzID) [16], post-column derivatization techniques such as the coupling of the Paterno Buechi reaction to mass spectrometry (PB-MS) [17, 18], Electron-activated dissociation (EAD) [19, 20] and ultraviolet-photodissociation (UVPD) [21]. These techniques do generate double bond specific fragments

for various class of lipids but do not allow to retrieve *sn*-positions within single MS2 experiments, except EAD [15]. More specific, EAD of sodium adducts of triglycerides generates unique fragments for fatty acids at *sn*2 and *sn*1/*sn*3 positions [19]. However, MS3 experiments allow to assign *sn*-positions and *sn*-specfic double bond positions of fatty acids by methods such as PB-MS3 or UVPD-MS3 of dioxolane (diacylglycerol) fragments generated by CID of sodium adducts of lipids. [22, 23].

Most techniques provide a gain in structural information but require elevated reaction times which challenges the compatibility with fast LC analyses. OzID [24], requires reaction times from 10-200 ms range (OzID at intermediate pressure, without precursor selection) to seconds (OzID in vacuum, with precursor selection). The experiment cycle time for EAD and UVPD does depend on the MS instrumentation. In the case of EAD, reaction times (typically 150msec) and accumulation times (approx. 1s) might be required for adequate reaction yields and signal-to-noise ratios of low abundant lipid species [19]. However, by compromising MS2 spectra quality a shorter accumulation time of can be used increasing the number of precursors that can be monitored in a single LC-run.[25]. This is critical for the analysis of complex biological samples, where chromatographic separation of isobaric and isomeric species is mandatory for unambiguous lipid identification. Analyses by gas chromatography with electron ionization (GC-EI-MS) of mono- and diglycerides as derivatives have been reported with improved double bond position specific fragmentation along with *sn*-positions related fragmentation but are limited to the molecular weight of the lipid [26]. For glycerolipids two main LC separation mechanisms are applied, either the compounds are separated by the carbon-chain length, number and position of double bonds (lipophilicity) using reversed-phase liquid chromatography or by their head group (hydrophilicity) using hydrophobic-liquid-interaction-chromatography [13]. Supercritical fluid chromatography (SFC) has also been demonstrated to be a powerful separation technique of nonpolar lipids, such as triglycerides [27]. Only a few studies investigated the utilization of APPI for lipidomic studies, but no radical cations were observed independent from ion-source, lamp type and MS instrument used [14, 28-30]. Instead, protonated molecules, ammonium adducts and in-source fragmentation like fatty acid and hydroxyl group losses were observed. Ion speciation in dopant-assisted APPI depends on analyte properties and ionization conditions, such as dopant molecule, mobile phase choices as well as their corresponding flowrates [31, 32]. Certainly, solvent-dopant combinations with typical LC solvents play the most prominent rule and can prevent ionization, allow radical cation formation or lead to predominant analyte protonation. Methanol as mobile phase in combination with halogenated benzenes, such as chlorobenzene, has

proven as superior combination for radical cation formation [33, 34]. We recently demonstrated that under well controlled µLC conditions with post-column addition of methanol, radical cations can be generated by chlorobenzene-assisted atmospheric pressure photoionization (APPI) of diverse compound classes including, steroids, isoprenoids and polyketides. In addition, CID fragmentation of radical cations generate EI like fragmentation spectra which can be utilized for EI library searches [34]. Similar to µLC with post-column addition, SFC with methanol as polar mobile phase additive is a suitable separation technique which allows to maintain radical cations generated by chlorobenzene-assisted APPI [35].

In the present work we investigate the application of APPI-MS with chlorobenzene as dopant for the formation of electron deficient precursors ($M^{+\cdot}$ and $[M-H]^+$) of acylglycerol and subsequent fragmentation by CID compared to spectra obtained from ESI-EAD. Based on the rational CID fragmentation of electron deficient precursors, a software tool for rule based de-novo annotation of double bond positions within acylglycerols was developed. Finally, the applicability of APPI-CID is demonstrated for the analysis of acylglycerols lipids by SFC-MS in linseed oil using data-dependent acquisition.

## EXPERIMENTAL SECTION

### *Chemicals*

Standard compounds were from Cayman, Larodan, Sigma-Aldrich, and Supelco (Table S1). Stock solutions were prepared in methanol, ethanol, toluene, chloroform or chlorobenzene. Methanol, ethanol and chloroform were from Fisher Chemical, chlorobenzene from Sigma-Aldrich, toluene from Carl Roth , ammonium formate from Honeywell Fluka and $CO_2$ 4.5 from PanGas. Linseed oil was from a Swiss supermarket (Alnatura Leinöl nativ, Migros, Geneva, Switzerland) aliquoted and stored at -20°C until use.

### *Supercritical Fluid Chromatography*

SFC was performed using a Nexera UC system (Shimadzu, Kyoto, Japan). Acylglycerol standards and linseed oil lipids were separated on a Viridis HSS C18 SB Column (Waters, 100Å, 1.8 µm, 3 mm x 100 mm) at 40°C using a gradient from 5% MeoH to 25% MeOH in 5.25 min and to 100% in 6 min with a washing step until 9 min for standards and adjusted for linseed oil with 10% to 25% MeOH in 5.25 min. The backpressure regulator was set to

10 MPa and 50°C. The total flowrate was set to 1 mL/min with a makeup flow rate of 200 µl/min for APPI and 50 µL/min for ESI. ammonium format 0.1 % (w/v) was added to MeOH for ESI analysis.

*Mass Spectrometry*

All samples were analyzed on a QqTOF (6600 TripleTOF, SCIEX, Concord, ON, Canada) equipped with an APPI source (PhotoSpray, SCIEX, Concord, ON, Canada) using chlorobenzene as dopant (20µL/min) or a ESI DuoSpray ion source (SCIEX, Concord, ON, Canada). The ion source settings for APPI and ESI are given in Table S2. All TOF-MS experiments were performed with an accumulation time of 100 ms. Collision-induced dissociation spectra of radical cations and ammonium adducted acylglycerol standards were acquired from 10 to 70 eV in steps of 5 eV with accumulation times of 50 ms. For Linseed oil analysis, data-dependent acquisition of the 10 highest ions was performed using a collision energy spread from 10-70 eV with accumulation times of 85 ms. All EAD experiments were performed on a ZenoTOF 7600 (SCIEX, Concord, ON, Canada) equipped with an ESI DuoSpray ion source using MRM-HR with an accumulation time of 62 ms, reaction time of 20 ms and a kinetic energy of 10 eV.

## RESULTS

### *Ionization of acylglycerols by APPI*

When using SFC-APPI-MS with chlorobenzene as dopant acylglycerol ion speciation is influenced by the number of double bonds. Acylglycerols without double bonds form predominant diacylglycerol fragments as well as less abundant monoacylglycerol and fatty acid fragment ions with almost no intact analyte ion present (Figure 1A, Supplementary Figures S1 - S3). With an increasing degree of unsaturation, combined with the distribution of double bonds across all fatty acids the intensity of intact odd-electron analyte ions increases (Figure 1B-F, Supplementary Figures S1-S8). Acylglycerols with ≤ 3 double bonds in total form $[M\text{-}H]^+$ ions from hydrogen radical abstraction (Figure 2B, Supplementary Figure S1, S4-S6) and in-source fragments with increasing contribution of $M^{+\cdot}$ for acylglycerols with ≥ 3 double bonds (Figure 1C-F, Supplementary Figures S1, S7, S8). Observed in-source fragments are sufficient to reconstruct given acylglycerols fatty acid composition. Intensity ratios of fatty acid, mono- and diacylglycerol fragments show characteristic changes based on the *sn*-positions of attached fatty acids and hydroxyl groups with preferred losses of *sn*1/*sn*3 substituents (Supplementary Figures S3-S8).

In the case of TG(18:3/18:3/18:3) m/z 803.6163 is observed, which represents an elemental formula loss of $C_5H_9$ and thereby a bond cleavage adjunct to the double bond position n-6 (Figure 1D, Supplementary Figures 8E-F). In the case of 2-arachidoniyl glycerol, (+)-ESI signals are distributed across 6 six different ions, including the protonated analyte, sodium and ammonium adducts as well as in-source fragments, while a dominant radical cation is formed when using APPI (Figure 1F, Supplementary Figure 7E). APPI has shown to be particularly useful for monoglycerides with a high degree of unsaturation which do not ionize well in (+)-ESI

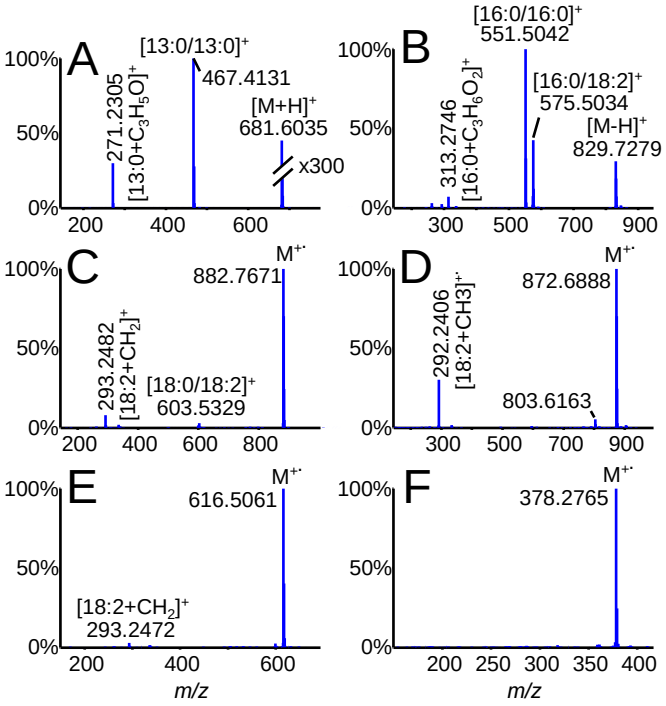


*Figure 1: SFC-APPI MS1 spectra of 6 mono-di and tri acylglycerol standards **A**, TG(13:0/13:0/13:0), **B**) TG(16:0/16:0/18:2), **C**) TG(18:2/18:0/18:2), **D**) TG(18:3/18:3/18:3), **E** DG(18:2/OH/18:2) and **F** MG(OH/20:4/OH)*

### *CID of unsaturated odd-electron ion acylglycerol precursors*

Triglycerides CID fragmentation of ammonium adducts, ionized with ESI, generally yield abundant diglyceride, monoglyceride and fatty acid fragments which allow to retrieve the fatty acid composition but fail to identify double bond positions [36]. Contrary, the CID fragmentation of unsaturated OE acylglycerol precursors yields information rich fragmentation spectra, with multiple fragments related to the fatty acid composition as well as double bond positions (Figure 2). Similar to EAD, odd electron precursors collision induced dissociation (OE-CID) does not rely on a small set of specific fragments and their corresponding mass differences but does generate fragments all along the alkyl chain of the fatty acid. In order to spot the double bond position it is necessary to

follow the fragmentation of $CH_3(CH_2)_n$ units until the maximal intense peak for a given series is reached. In the case of triolein (OOO) $[M-H]^+$, this corresponds to a bond breakage adjunct to the double bond leading to an loss of $CH_3(CH_2)_7$ which indicates the presence of the double bond position n-9 (Figure 2A). The $CH_3(CH_2)_n$ series does not stop, as expected at the double bond, due to radical and double bond migrations similar to fragmentation observed in EI [37]. Additional $CH_3(CH_2)_n$ series are observed after a variety of bond dissociation events, including the loss of fatty acids or hydroxyl groups, and can be used for complementary double bond position confirmation. More pronounced for radical cations than for $[M-H]^+$ ions is that diacylglycerol, monoacylglycerol, and fatty acid fragments show a variety of fragments related to a single fatty acid which differ by hydrogen count and intensities. These hydrogen differences generate characteristics patterns, which are related to the double bond composition of acylglycerols (Supplementary Figure S9-S336). Among these, the most abundant fragments differ by several hydrogens from those obtained through CID fragmentation of ammonium adducted acylglycerols, indicating the formation of different fragment ions between OE-CID and EE-CID. Very similar fragmentation patterns are observed for polyunsaturated fatty acids. The first double bond position is tracked by the $CH_3(CH_2)_n$ elemental formula loss series, whereas the second double bond positions includes the loss of the first double bond (CH=CH) which induces a ΔH2 shift. In the case of trilinolein (LLL) this allows to assign the first double bond position to n-6 and the second double bond position to n-9 (Figure 2B). Moreover, double bond specific fragments for LLL are higher than for OOO. While in general, the $CH_3(CH_2)_n$ $(\Delta H2)_x$ elemental formula loss series are the most dominant fragmentation series, additional series with odd hydrogen number differences are observed and can be used for additional verification (Figure 2C, Supplementary Figure S9-S336). Additional fragmentation patterns of the alkyl chain of fatty acids are observed with and without retention of oxygen or the carboxyl group.. Certainly, if at least one oxygen remains attached fragmentation has to occur from the aliphatic end of the fatty acid. After the loss of the carboxy group, fragmentation could happen from both sides which may generate overlapping fragmentation series (Figure 2C).

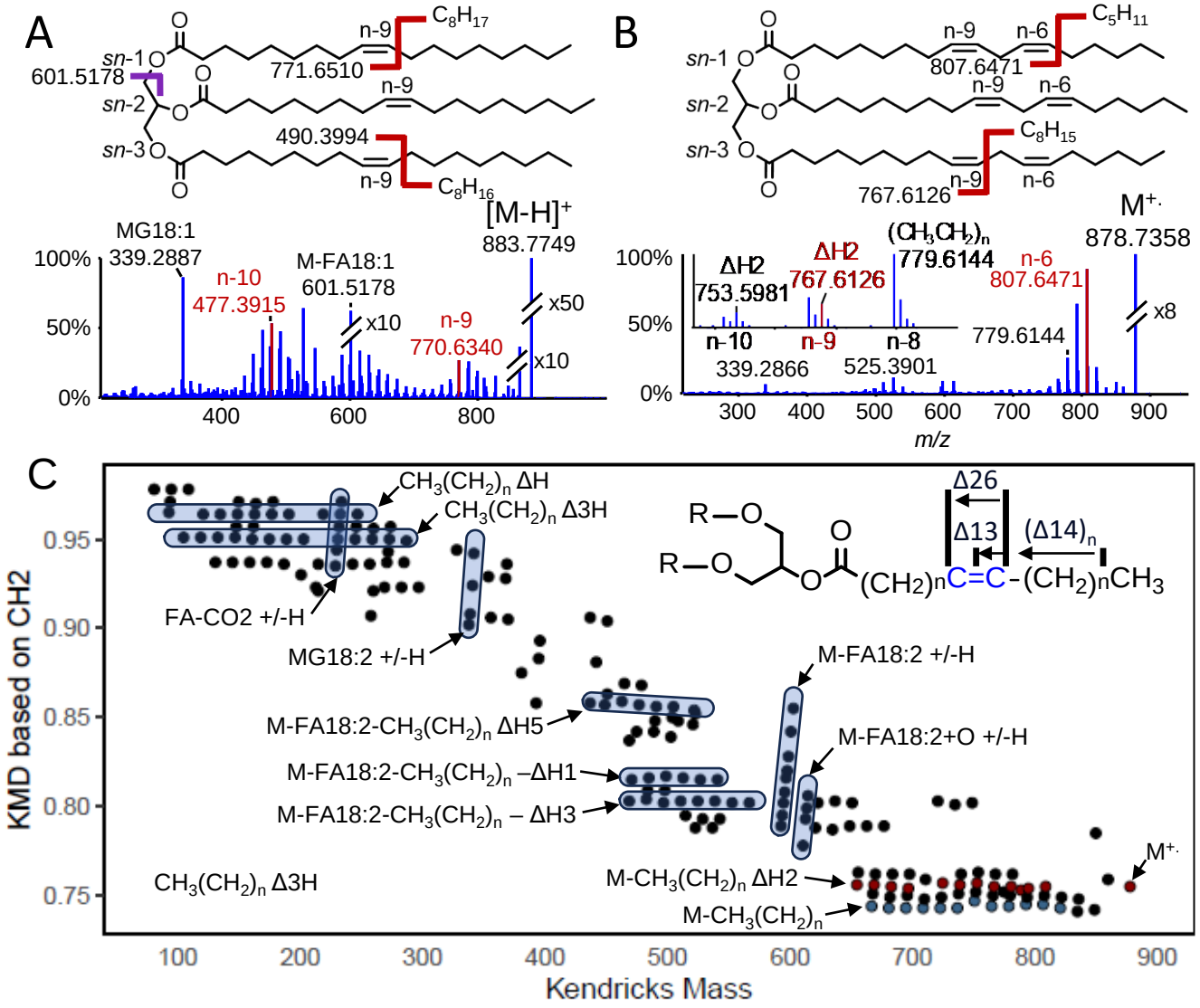


*Figure 2:* *35 eV CID of A) OOO $[M-H]^+$ and B) LLL $M^{+\cdot}$ with C) the Kendricks plot of 35 eV CID of LLL radical cation· with intensities above 10 counts and an minimum relative intensity of 0.1%. Red lines indicate the maximal intense fragments and thereby the start of a double bond of each double bond specific elemental formula loss series. The inset of B) shows an zoom onto the double bond specific elemental formula loss series of position n-9.*

***Double Bond Position Assignment using MsRadaR***

Fragment rich spectra of OE-CID makes manual double bond assignment tedious. We developed MsRadaR an R package with a de-novo structural elucidation pipeline (Figure 3A). MsRadaR requires a centroided mass spectrum as input and can be used to retrieve elemental formula losses (EFL) from defined starting points, such as the precursor mass or M-FA. EFL are utilized to extracts relevant $(CH_3CH_2)_n\,\Delta H_x$ series and performs maximal intensity peak picking to annotate double bonds. As a reference, MsRadaR calculates the loss of saturated fatty acids with successive $CH_3(CH_2)_n$ losses and calculates the corresponding hydrogen differences of the given mass spectrum. Double bonds are expected to induce a Δ2H shift for each double bond (Figure 3B). Finally, MsRadaR allows to navigate through fragmentation spectra of OE acylglycerol precursor CID by visualizing and summarizing each fragmentation series (Figure 3C). The rational fragmentation of OE precursors can be applied to a wide variety of tri- and diglycerols independent from the selected OE ion precursor ($M^{+\cdot}$ and $[M\text{-}H]^+$) (Figure 3C). False annotation can be prevented by including additional measures for double bond annotation, considering the intensity slope (Supplementary Figure S9-S336) and/or additional double-bond specific fragmentation series such as M-FA-$(CH_3(CH_2)_n\,\Delta 2H_x$ (Supplementary Figure S337-338). The intensity slope is in most cases maximal at the double bond position and accompanied by a sign change, with a minima, 1-2 carbons after the double bond position. For 1,3-dilinoleoyl-2-stearoyl glycerol (LSL) the intensity slope shows that the first double bond is at position n-6 and minimal at position n-9, alike the M-FA-$(CH_3(CH_2)_n\,\Delta 2H_x$ fragmentation series (Supplementary Figure S337-338).

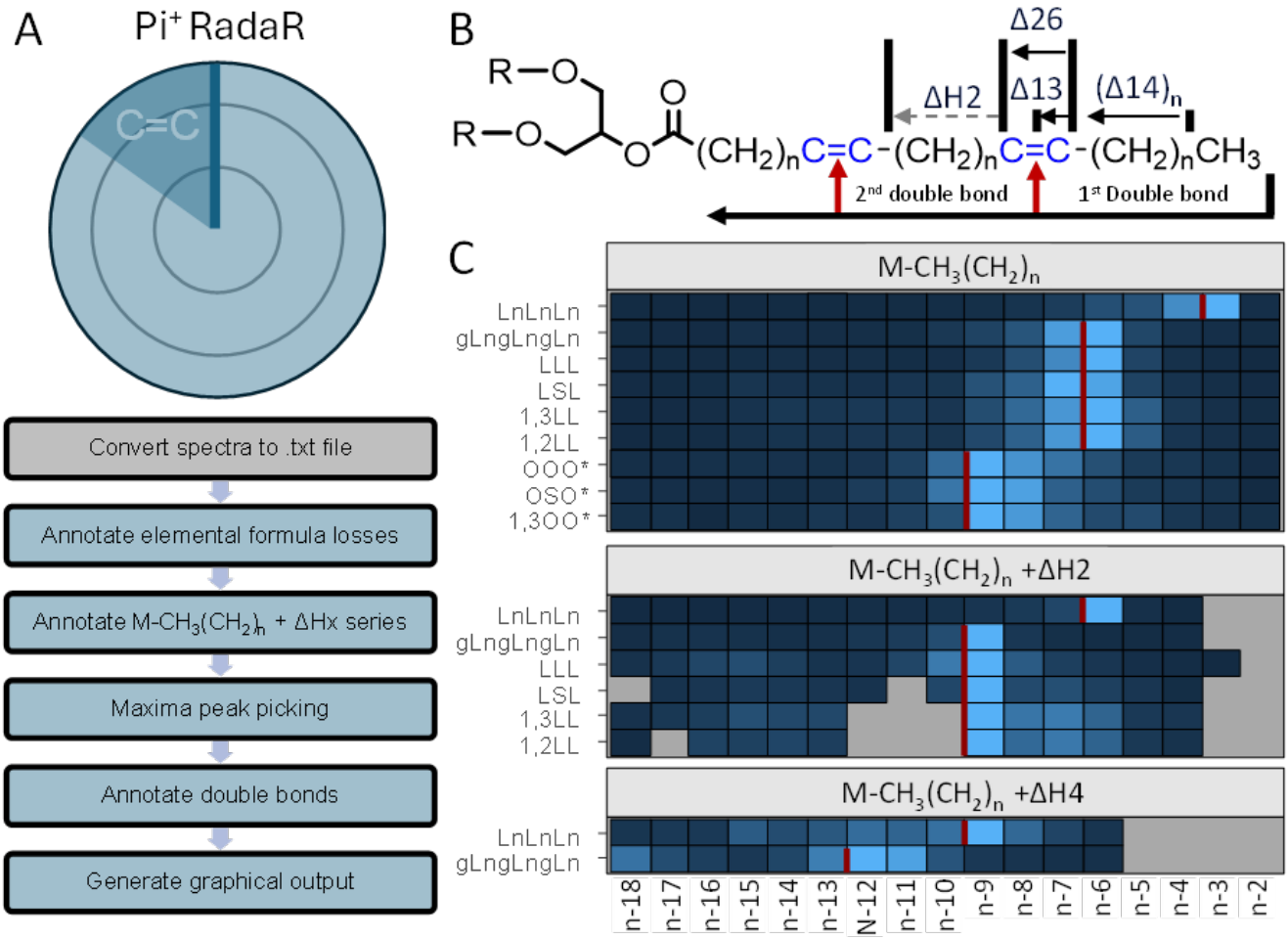


*Figure 3: Automated annotation of double bond positions using the MsRadaR R package. A) MsRadaR workflow, B) Fragmentation scheme of acylglycerols, C) graphical summary of MsRadaR results for a set of 9 acylglycerols. Colorscale of the heatmap represent relative intensity per series and analyte with 0% (darkblue) to 100% (lightblue). Grey cells represent missing values and red lines double bond positions. L: linoleic acid, S: stearic acid, Ln: α-linolenic acid, gLn: γ-linolenic acid, O : oleic acid.*

***OE-CID fragmentation and annotation of acylglycerol with mixed fatty acid chains***

Acylglycerols with 2 or more unsaturated fatty acids with varying double bond positions generate overlapping fragmentation series. In that case, double bonds can be assigned based on the occurrence of one maxima per unique double bond position. For the regioisomeric triglycerides 1-oleoyl-2-palmitoyl-3-linoleoyl-glycerol (OPL) and 1-palmitoyl-2-linoleoy-3-oleoyl-glycerol (PLO) and diglyceride 1-oleoyl-2-linoleoyl-glycerol (OL), the first double bond of FA18:2 generates a small maxima indicating position n-6 followed by a second maxima from fatty acid FA18:1 at carbon position n-9 (Figure 4A-C). The use of intensity slopes allows to mitigate the masking of overlapping fragmentation series (Figure 4D-F). For all three acylglycerols the intensity slope shows two

maxima after 5 and 8 carbon losses, followed by two sign changes alongside 2 minima after 6 and 9 carbon losses, indicating the first double bond positions as n-6 for FA18:2 and n-9 for FA18:1. The second double bond with carbon position n-9 of FA18:2 generates a slope maxima after 8 carbon losses, followed by either missing signals for the triglycerides or a sign change with a minima after 9 carbon losses for the diglyceride. In addition to the intensity slope maxima related to the double bond position n-9, another intensity maxima after 5 carbon losses for the triglycerides and 6 carbon losses for the diglyceride OL are observed. These are most likely caused by the isotopic contribution of the M-$CH_3(CH_2)_n$ ΔH series from almost equally intense $[M-H]^+$ ions (Figure S6D-G). Despite double bond related fragment ions, pronounced diacylglycerol, monoacylglycerol and fatty acid fragments can be observed. It is to expect, that the isotopic contribution of $[M-H]^+$ ions is the major origin of these fragment ions. In general intensity ratios changes are observed for regio isomeric acylglycerols. If a saturated fatty acid is situated on *sn*-position 2, a dominant cleavage between the alpha carbon of the fatty acid and the oxygen of the glycerol backbone is observed (*m/z* 617.5141). If situated at *sn*-position 1/3, the fatty acid loss predominantly leads to a cleavage between the glycerol moiety and the carboxy group of the fatty acid (*m/z* 600.509). This suggests that the ratio of *m/z* 617/600 can be used to assign saturated fatty acids either to *sn*2 or *sn*1/3 positions. This is not the case for unsaturated fatty acids which show altered fragmentation ratios at *sn*-2 positions (Supplementary Figure S9-S336). In addition, after the loss of FA18:0 from a triglyceride and OH loss in the case of a diglyceride, a second double bond fragmentation series appears with a very similar fragmentation pattern to M-$CH_3(CH_2)_n$ ΔxH loss series from the triglyceride or diglyceride precursor.

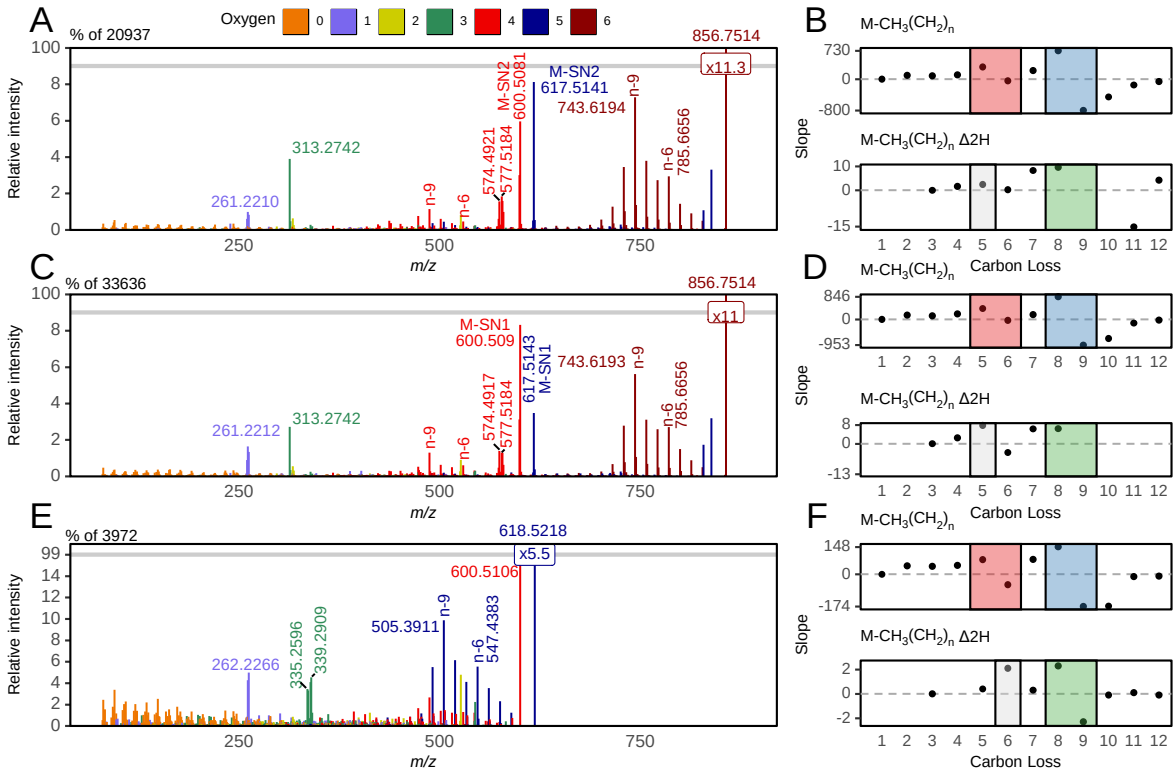


*Figure 4: Annotated 35 eV CID spectra using MsRadaR of A) OPL with B) extracted elemental formula loss series, C) PLO with D) extracted elemental formula loss series and E) OL with F) extracted elemental formula loss series. Red boxes indicate double bond position n-6 of FA18:2, blue double bond position n-9 of FA18:1, green double bond position n-9 of FA 18:2 and grey the isotopic contribution from M-$CH_3(CH_2)_n$ ΔH of the CID fragmentation of $[M-H]^+$ . For mass spectra, grey lines indicate breakpoint of the y-axis.*

***OE-CID fragmentation and annotation of acylglycerols carrying only one unsaturated fatty acid***

Intensities of double bond related fragmentation series depend on a variety of factors, such as amount of double bonds, amount of unsaturated fatty acids, amount of hydroxyl groups, collision energies and choice of ion species. Indeed, for monoacylglycerols lower collision energies are required (15-20 eV) than for diacyl- and triacylglycerols (35 eV) (Supplementary Figure S9-S336). For acylglycerols with only one unsaturated fatty acid, M-$CH_3(CH_2)_n$ ΔxH series are less pronounced and might not be sufficient to annotate all double bond positions. For instance, a triglyceride with two FA18:1 does show M-$CH_3(CH_2)_n$ ΔxH series (Figure S257-S266), while a triglyceride with one FA18:2 does not (Supplementary Figure S135-S144). This implies that saturated fatty acids and hydroxyl groups are good leaving groups and that some isobaric acylglycerols (e.g. SLS and OSO) produce different fragmentation spectra) and different double bond related fragmentation series can be used to pinpoint double bond positions. In the case of MG18:2, after loss of the glycerol headgroup including the carboxy group of the fatty acid alongside an additional hydrogen $[M\text{-}C_4H_7O_4\text{-}H]^+$, double bond fragment series dominate, (Figure5) allowing to assign double bond positions n-6 and n-9 for MG18:2. Similar fragmentation series are observed for tri- and diglycerides carrying FA18:2 at a collision energy of 35 eV (Supplementary Figure S9-S336).

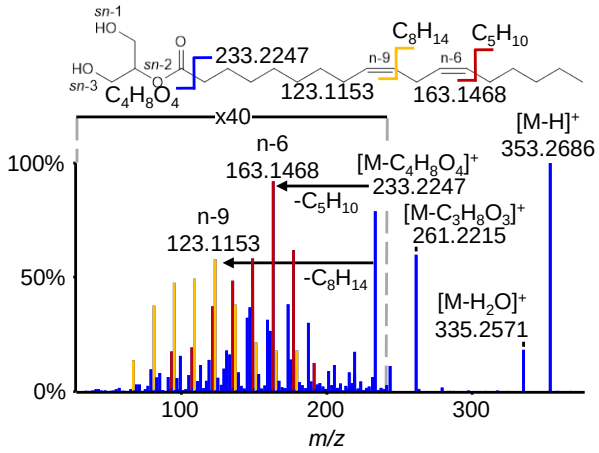


*Figure 5: Product ion spectrum at 15 eV of the $[M\text{-}H]^+$ ion of MG(OH/18:2/OH). Red bars indicate $[M\text{-}C_4H_8O_4\text{-}CH_3(CH_2)_n]^+$ loss series, yellow bars indicate $[M\text{-}C_4H_8O_4\text{-}CH_3(CH_2)_n\,\Delta 2H]^+$ loss series.*

***Comparison of Electron Activated Dissociation of Even-Electron Precursor Compared and Odd-Electron Precursor CID***

The OE-CID (radical cation) and EAD spectra (sodium adduct) of the regioisomeric triglycerides TG(16:1/16:1/18:1) and TG(16:1/18:1/16:1) are presented in Figure 6 A to D. The double bond positions n-7

and n-9 can be retrieved by spotting Δ26 (CH=CH) (Figure 6A and 6C) or Δ12 (Figure 6C) differences caused by the loss of a double bond, and *sn*1/3 and *sn*2 specific fragments. For EAD it is not possible to obtain the stoichiometry of double bond positions n-7 and n-9, nor to assign double bond positions to fatty acids FA16:1 or FA18:1. OE-CID shows better signal-to-noise (S/N) ratio for double bond related fragments but is less specific for *sn*-positions and relies on fragment intensities ratios of diacylglycerol, monoacylglycerol and fatty acid fragments (Figure 6B-D, Supplementary Figure S9-S336). While affected by the stoichiometry of fatty acids, diacylglycerol fragments with *sn*1/3 losses are preferred over *sn*2 losses, creating dominant *sn*2 positional monoacylglycerol fragments. In addition, for acylglycerols which do carry FA16:1(n-7) and 18:1(n-9) overlapping EFL series are formed. In this case, M-$CH_3(CH_2)_n$ series for de-novo annotation are less accurate, as the FA16:1 (n-7) fragment dominate (Figure 6B-D-E). M-$CH_3(CH_2)_n$ series after fatty acid loss (FA16:1 and FA18:1) allow systematic double bond position assignment, retrieve the stoichiometry of double bonds and assign double bonds to specific fatty acids in four steps (Figure 6E-F-G). First, M-$CH_3(CH_2)_n$ series are evaluated for intensities slopes, which allows to enclose potential double bond positions between the carbon positions n-6 and n-9 due to an intense peak at position n-8 (Figure 6E-F). Second, M-FA-$CH_3(CH_2)_n$ series of FA16:1 and FA18:1 ( *m/z* range 350-550) intensity maxima are used to locate potential double bond positions. For M-FA16:1-$CH_3(CH_2)_n$ of TG(16:1/16:1/18:1) which indicates n-7/n-9 and for TG(16:1/18:1/16:1) n-9 as potential double bond positions. Third, potential double bonds from M-FA-$CH_3(CH_2)_n$ are excluded based on estimated double bond regions from M-$CH_3(CH_2)_n$ series (Figure 6E-F). This allows to neglect n-5 as potential double bond position, as there is no indication for position n-5 within the M-$CH_3(CH_2)_n$ elemental formula loss series and stems from the shifted n-7 position from M-FA16:1-$CH_3(CH_2)_n$. Fourth, potential combinations of FA16:1, FA18:1 and n-7/n-9 losses are considered and compared to the M-$CH_3(CH_2)_n$ and M-FA-$CH_3(CH_2)_n$ loss series (Figure 6E-F-G). Last, we observe sn-position related intensity alterations of the M-FA-$CH_3(CH_2)_n$ series, which can be logically explained by the intensity ratios of M-FA16:1(n-7) and M-FA18:1(n-9) diacylglycerol fragments. For TG(16:1/18:1/16:1), the M-FA16:1 diacylglycerol fragment is 1.18 times higher, leading to a masked intensity maxima at n-7 and a more dominant intensity maxima at position n-9 for the M-FA16:1-DB series. Contrary, for TG(16:1/16:1/18:1), the M-FA18:1 diacylglycerol fragment is 4.55 times higher, which leads to two distinguishable intensity maxima with n-7 from the M-FA16:1 series a pronounced intensity maxima at n-7 for the M-FA18:1-DB series. This implies, that the M-FA-$CH_3(CH_2)_n$ series creates an unique fingerprint which will be different for any acylglycerol, in-

cluding regio- and double bond positional isomers. The combination of all these steps enables only for OE-CID to confirm the stoichiometry and position of double bonds as well as the fatty acids composition for the two regioisomeric TG(18:1(n-9)/18:1(n-9)/16:1(n-7)) and TG(18:1(n-9)/16:1(n-7)/18:1(n-9)).

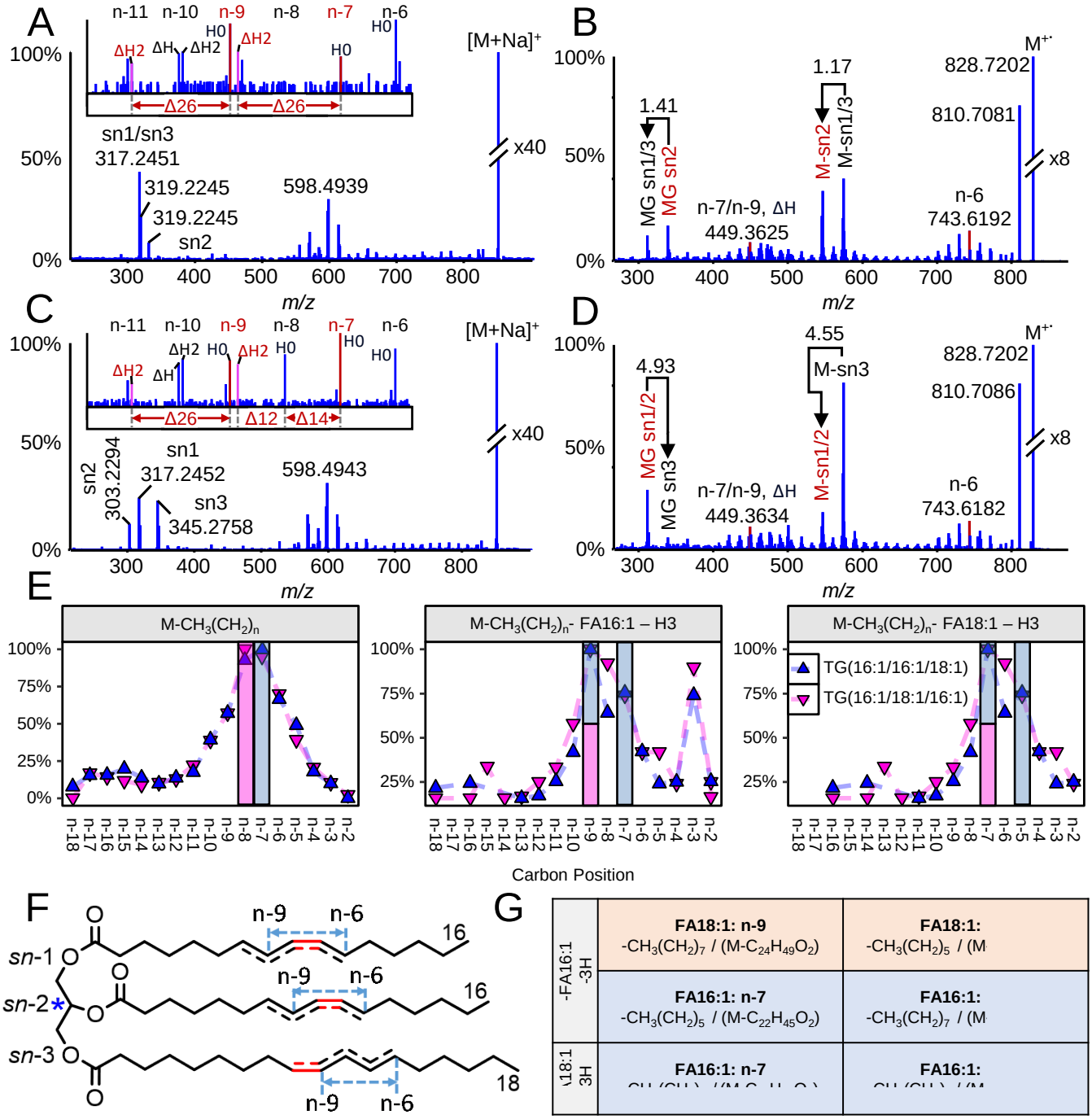


*Figure 6: Product ion spectra of regioisomeric TG(18:1(n-9)/18:1(n-9)/16:1(n-7)) using A) EAD of the sodium adduct or B) CID of the radical cation and TG(18:1(n-9)/16:1(n-7)/18:1(n-9)) using C) EAD of the sodium adduct or D) CID of the radical cation. Insets of EAD spectra reflect a zoom onto the double bond specific fragmentation series. E) Extracted elemental formula series of radical cation CID of both regioisomers, where red lines indicate the double bond positions. F) Triglyceride with potential double bond positions. Red color indicates true double bond position. G) Combinatorial possibilities of losses indicative for putative double bond positions with orange for FA18:1 and blue for FA16:1.*

***SFC-APPI-CID acylglycerol analysis of linseed oil***

High-resolution mass spectrometry with supercritical fluid chromatography and a HSS C18 column along with APPI is well suited for the separation of acylglycerols and acylglycerol double bond positional isomers and allowed to identify 38 different acylglycerols as radical cation (Figure 7A, Table S3). Among these, 31 are triglycerides 5 are diglycerides and one is a monoglyceride. Differences in collision energy required for a variety of structural informative fragments across different acylglycerol classes suggests the use of collision energy ranges (e.g. 10-70 eV) or energy stepping for the identification of unknown acylglycerols with standards (Figure 7B). The CID fragmentation (10-70eV) of the radical cation of the precursor TG57:9 at *m/z* 872.6888 (RT = 3.4 min) can be identified by comparison with standard triglycerides acquired at 40 eV (Figure 7B-C). Clear differentiation of the double bond positional isomer carrying three times FA18:3 with n-6,n-9,n-12 is possible by de-novo structural elucidation or library matching paired with retention time similarities of standards. This allows to annotate the TG57:9 as TG(18:3/18:3/18:3) with double bond positions n-3,n-6,n-9 for all 3 FA18:3.

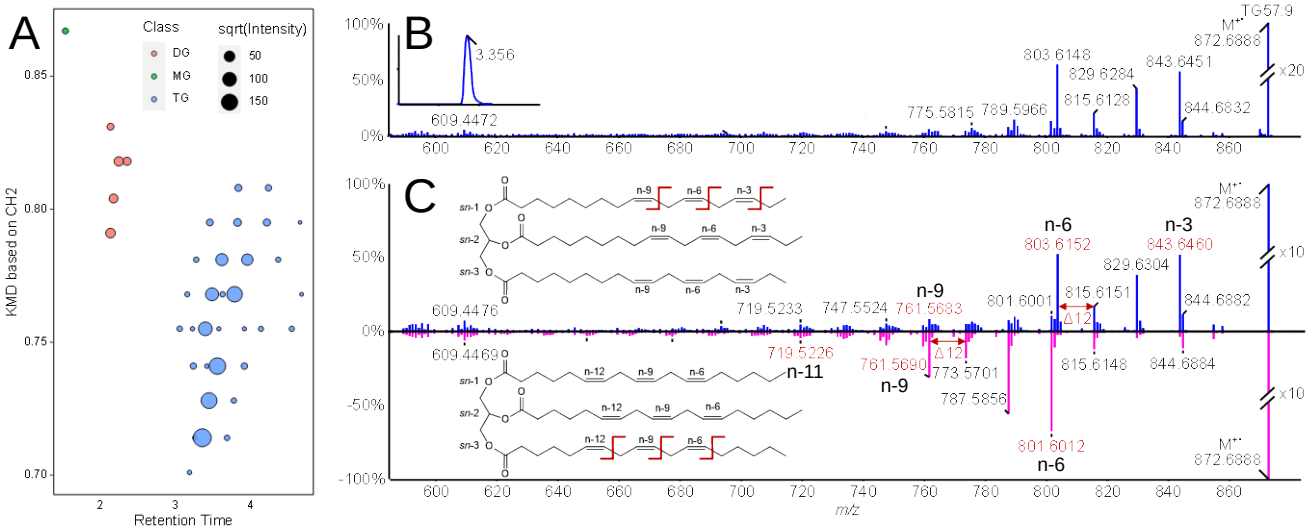


*Figure 7: A) Filtered Kendricks mass defect plot of acylglycerols (n=38) found in linseed oil as radical cations and B) 10-70 eV Collision-induced dissociation spectra of an unknown triglyceride at RT 3.4 min compared to two 40 eV spectra of isomeric triglycerides with 1,2,3-tri-α-linolenoyl glycerol and 1,2,3-tri-γ-linolenoyl glycerol.*

***SFC-APPI-CID analysis of fatty acids***

SFC-APPI-OE-CID analysis of FA18:3(n-3,n-6,n-9) follows similar fragmentation rules, for the first double bond position as presented in Figure 8. However, the following double bond positions are annotated on a different bases and is related to the ionization site of the radical cation, leading to M-$CH_3(CH_2)_{n-1}$ series with odd delta hx counts. In that sense, the first double bond position is found with the M-$CH_3(CH_2)_{n-1}$ series indicated by the maximum after 2 carbon losses. Fragmentation continues with a maximum for the M-$CH_3(CH_2)_{n-1}$ ΔH series at the double bond position after 3 carbon losses. Afterwards, the M-$CH_3(CH_2)_{n-1}$ Δ2H series starts, yielding a maximum after 8 carbon loses indicating the 3rd double bond position, instead of the second. The second double bond position is instead spotted by following the M-$CH_3(CH_2)_{n-1}$ Δ3H series. Additional structural information can be retrieved from the M-$CH_3(CH_2)_{n-1}$ Δ4H and M-$CH_3(CH_2)_{n-1}$ Δ5H series. Certainly, this shows that double bond related fragmentation series are produced for fatty acids, but that slightly different interpretation is required.

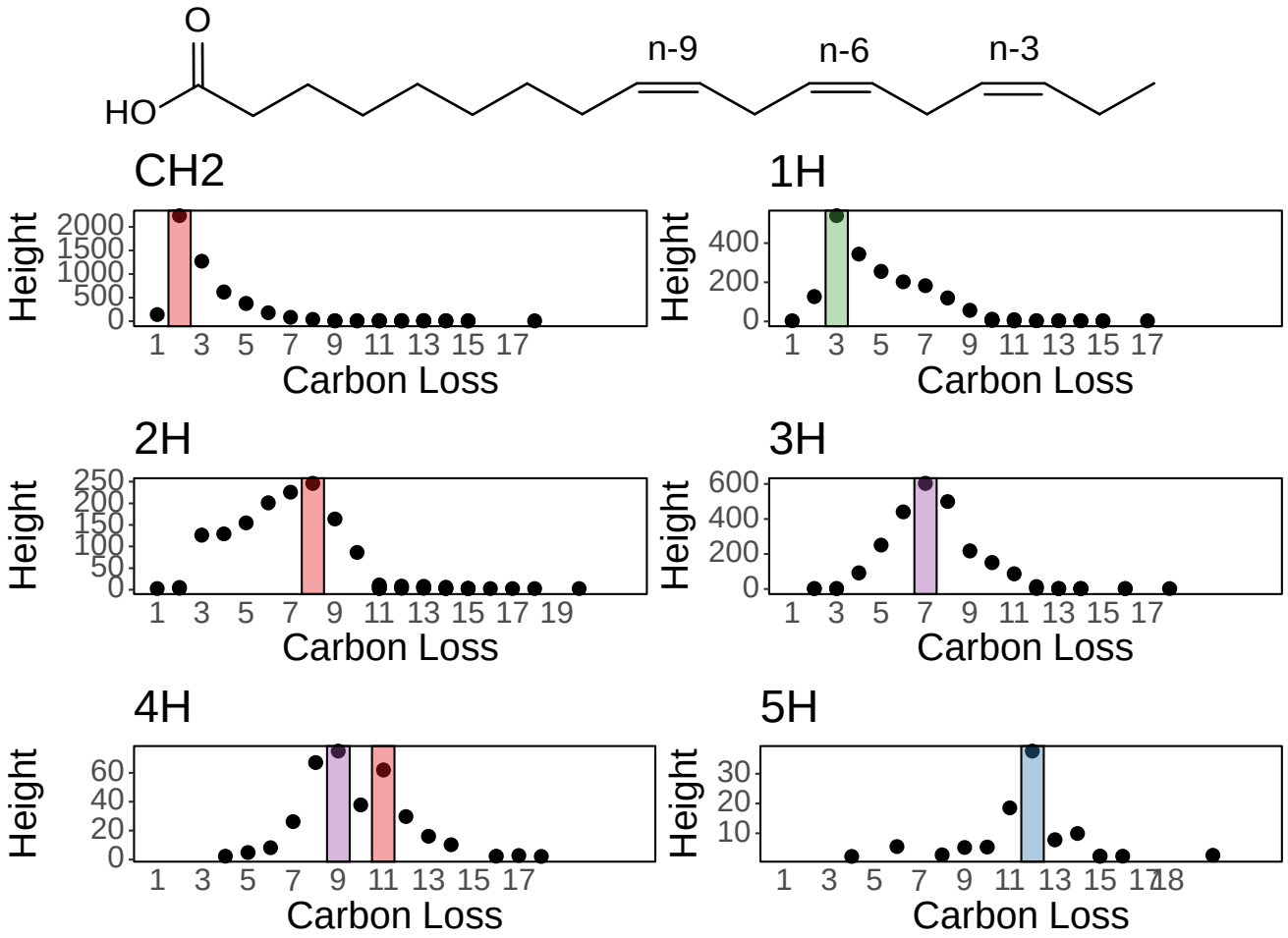


*Figure 8: SFC-APPI-OE-CID (20 eV) spectra interpretation of FA18:3(n-3,n-6,n-9) using MsRadaR*

***SFC-SWATH-APPI for untargeted lipidomics***

The capability to separate regio and double bond positional isomers with SFC allows to utilize data-independent SWATH acquisition for untargeted lipidomic analysis. For the double bond positional isomeric triglycerides 1,2,3-tri-α-linolenoyl glycerol and 1,2,3-tri-γ-linolenoyl glycerol, this allows to use extracted ion currents of specific double bond fragments for identification.

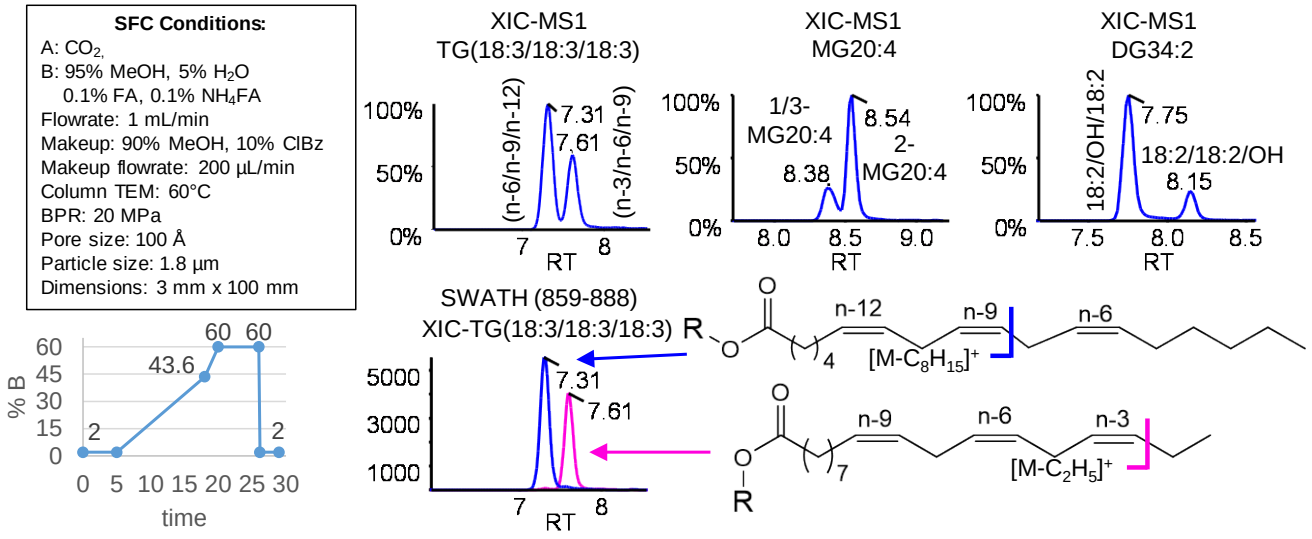


*Figure 9. SFC-APPI-SWATH CID experiments with a collision energy range from 10-50 eV of lipid standards with corresponding extracted ion currents. The chromatography method is adapted from Broughton, R., et al.*

***SFC-SWATH-APPI for the analysis of cholesteryl esters***

Similair to acylglycerols, untargeted swath analysis with SFC-APPI-OE-CID allows to annotate cholesteryl esters, such as CE20:4. Important to note is, that the alkyl chain the cholesterol (C8H17) will be present in every spectra and creates an additional maxima within the M-$CH_3(CH_2)_{n-1}$ series. Moreover, isotopic contributions might shift intensity maxima.

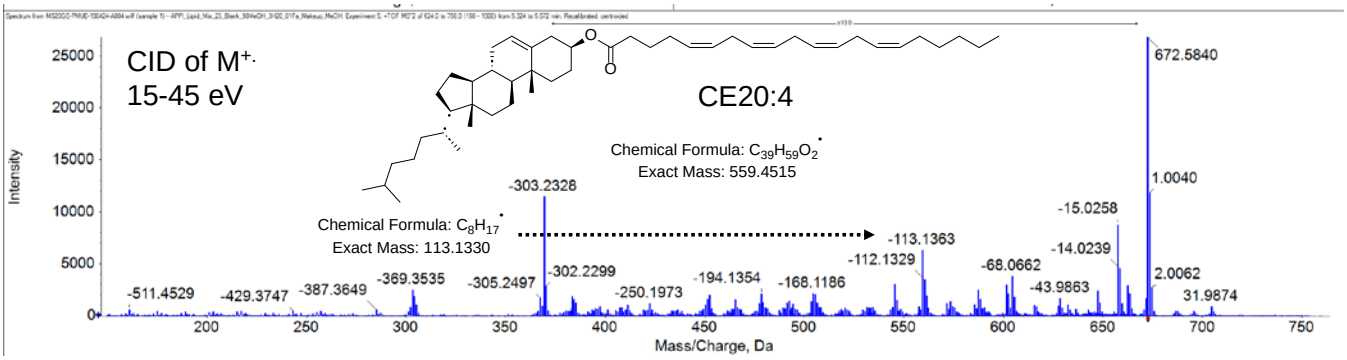


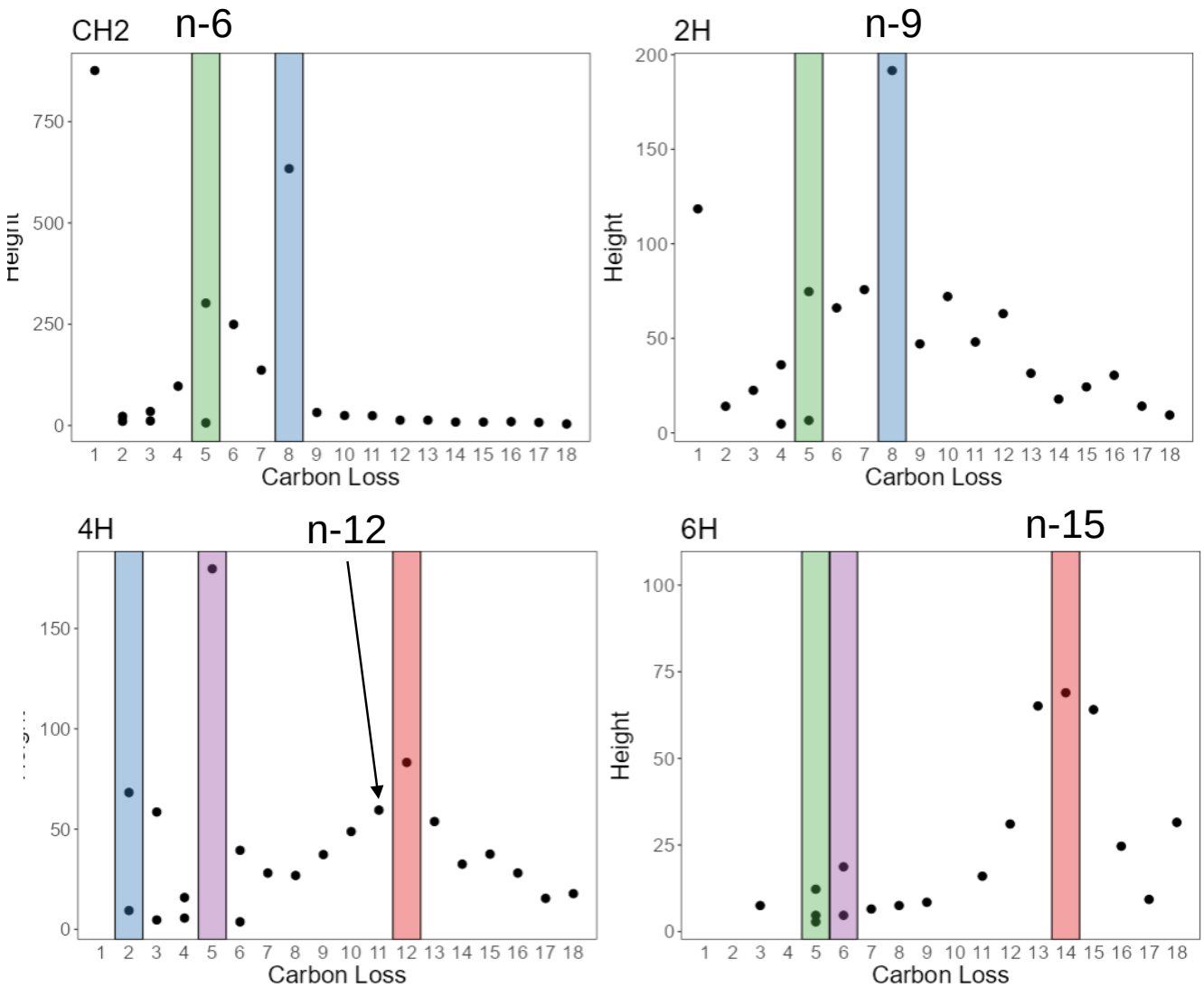

*Figure 10: SFC-APPI-OE-CID (10-45 eV) spectra interpretation of CE20:4(n-6,n-9,n-12,n-15) using MsRadaR*

***Targeted Lipidomic Analysis using Odd-Electron CID on a triple quadrupole linear ion trap ($QqQ_{LIT}$)***

The rational fragmentation of OE-CID allows to combine the sensitivity and selectivity of low resolution instruments for lipid characterization. For example, $QqQ_{Lit}$ instruments with selected reaction monitoring as survey scan followed by enhanced product ion scans as dependent scans allow targeted de-novo structural elucidation of lipids with MsRadaR for data visualization and interpretation.

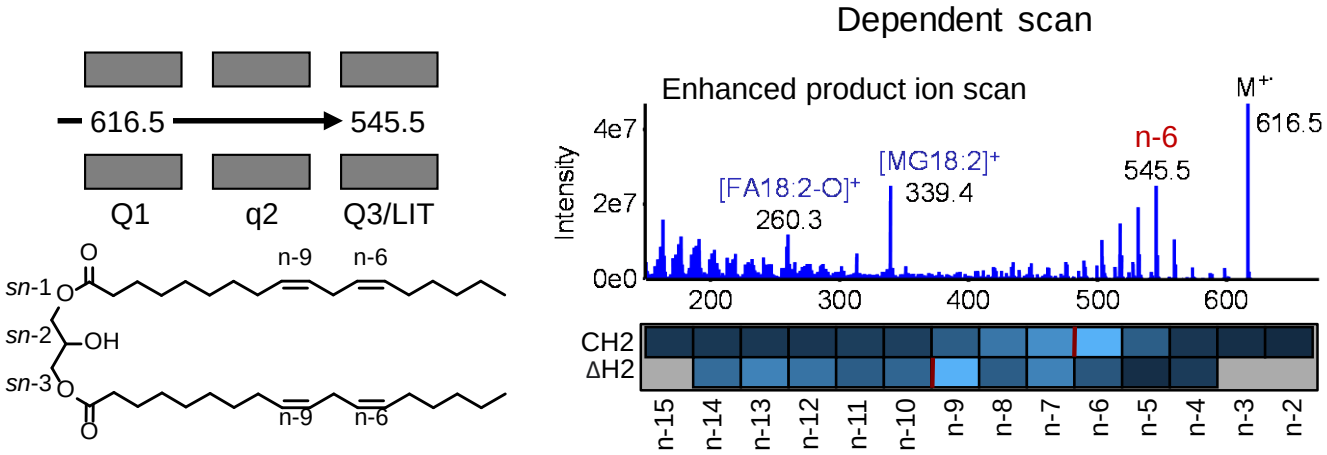


*Figure 11: SRM-EPI (CE: 35 eV) experiment of an unknown DG34:4 in human plasma extracted using the Matyash MTBE protocol with the first double bond position as Q3 transition and corresponding de-novo structural elucidation using MSRadaR's low-resolution double bond annotation functionality.*

***Odd-Electron CID vs Electron-Activated Dissociation of TG52:3***

OE-CID and EAD show orthogonal fragmentation spectra and can be interpreted using MsRadaR. OE-CID shows superior responses for double bond related fragment ions. In the case of TG(18:1/16:0/18:2) $[M+NH_4]$ EAD, double bonds are spotted by intensity drops of the $M\text{-}CH_3(CH_2)_{n-1}$ series and the start of Δ2H elemental formula loss series, caused by double bond losses.

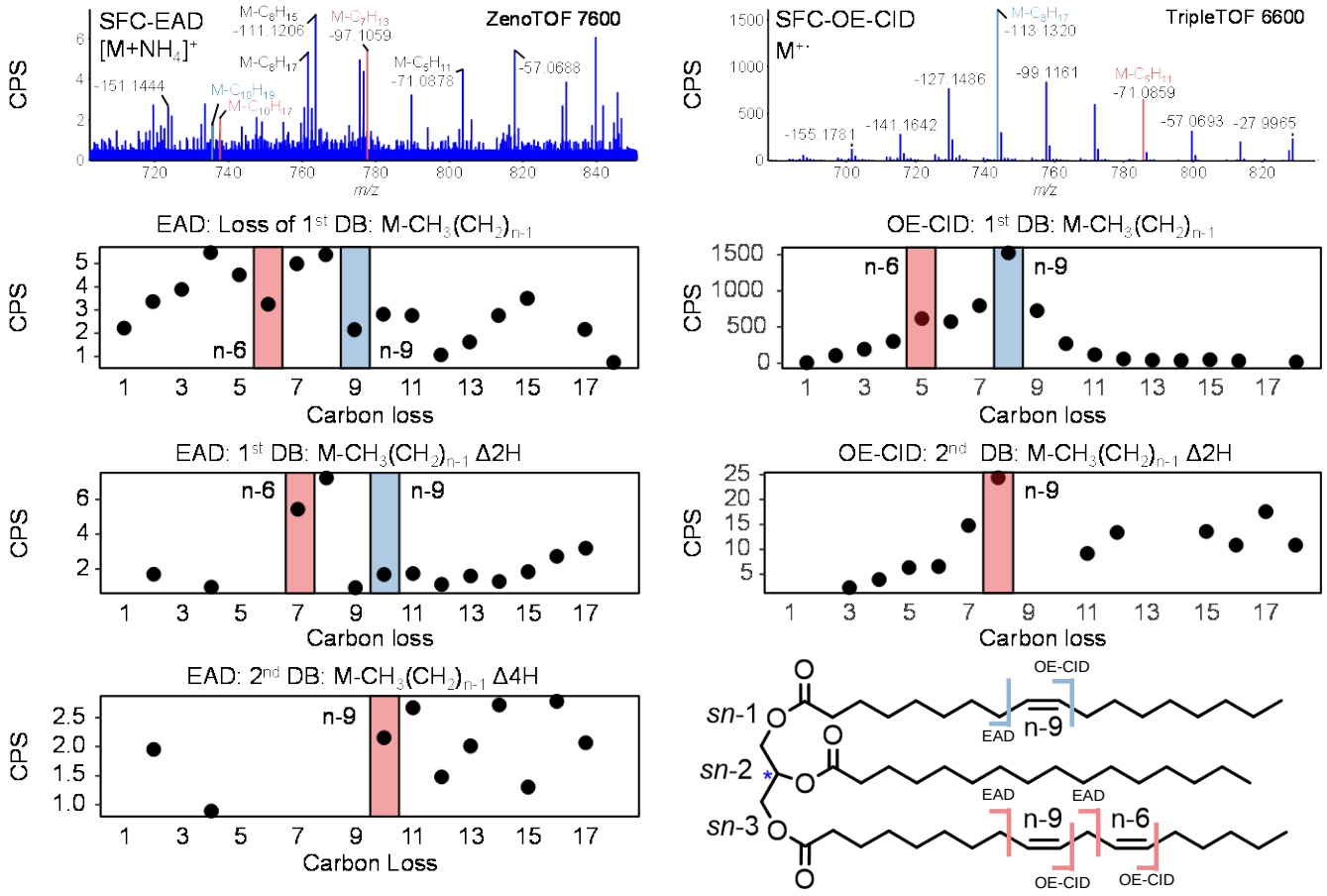


Figure 12: Product ion spectra and annotation of TG(18:1/16:0/18:2), Left panel EAD, Right panel OED-CID

## CONCLUSIONS

SFC allows the rapid separation of acylglycerol isomers in linseed oil in less than five minutes and with chlorobenzene assisted APPI-MS subsequent formation of odd-electron acylglycerol ions ($M^{+\cdot}$ and $[M-H]^+$). OE-CID of acylglycerols yields information rich fragmentation spectra with distinct intensity ratios for *sn*-positional isomers and multiple fragmentation series related to the double bond position of acylglycerols. For acylglycerols investigated (n=34), the most prominent fragmentation series starts directly from the precursor with successive losses of $CH_3(CH_2)_n$ units for the first double bond and additional Δ2H for each following double bond ($M\text{-}CH_3(CH_2)_n$ $\Delta 2H_x$). For additional fragmentation series, double bond positions can be spotted by defining the start of the series and spotting the corresponding intensity maxima of loss series, such as $[M\text{-}FA\text{-}3H\text{-}CH_3(CH_2)_n]^+$. Mixed fatty acid chain acylglycerols do generate overlapping fragmentation series, with one intensity maxima per unique double bond position. To overcome complex manual annotation of double bonds we developed MsRadaR and R-package with integrated data-processing workflows for double bond fragmentation series extraction and annotation. The approach is based on intensity maxima and intensity slopes and is applicable for spectra generated by EAD or OE-CID of acylglycerols. Unlike EAD fragmentation, OE- CID generates spectra with unique *sn*-postion related double bond fragmentation series which allow to assign double bonds to specific fatty acids and retrieve the corresponding stoichiometry from double bond fragmentation series after fatty acid losses ($[M\text{-}FA\text{-}3H\text{-}CH_3(CH_2)_n]^+$). Noteworthy, this is the first described methodology which does not require MS3 experiments to generate *sn*-releated double bond fragments. In addition, these fragmentation series represent unique fingerprint which will be different for any acylglycerol, including regio- and double bond positional isomers, which could be used for (in-silico) library matching with structure-based spectra prediction or evaluated using machine learning algorithms. Conclusively, odd-electron CID provides as powerful alternative for the structural elucidation of acylglycerols with better S/N ratio and shorter MS cycle times (e.g. 10-25 ms for a QqTOF) than methods such as EAD and UVPD. Generated product ion spectra are complementary to all existing techniques and rely on fragmentation series instead of single fragment pairs, which significantly increases the confidence in double bond annotation. Additional benefits of APPI-OE-CID are that neither dedicated instrumentation nor derivatization is required. The application of OE-CID for other lipid classes is shown as well the potential of data dependent acquisition using selected reaction monitoring mode as survey scan and enhanced product ion as dependent scan.

## SUPPORTING INFORMATION

List of analytes, MS-Source conditions, APPI and ESI MS/MS spectra of all acylglycerol standards and corresponding extracted series.


## ACKNOWLEDGMENTS:

The project was supported by the Swiss National Science Foundation under Project 200021_192306.

## REFERENCES


1. Mao, Y., et al., *Preparation, acyl migration and applications of the acylglycerols and their isomers: A review.* Journal of Functional Foods, 2023. **106**.
2. Kolczynska, K., et al., *Diacylglycerol-evoked activation of PKC and PKD isoforms in regulation of glucose and lipid metabolism: a review.* Lipids Health Dis, 2020. **19**(1): p. 113.
3. Baggelaar, M.P., M. Maccarrone, and M. van der Stelt, *2-Arachidonoylglycerol: A signaling lipid with manifold actions in the brain.* Prog Lipid Res, 2018. **71**: p. 1-17.
4. Missaglia, S., et al., *Neutral Lipid Storage Diseases as Cellular Model to Study Lipid Droplet Function.* Cells, 2019. **8**(2).
5. Weigel, C., et al., *Epigenetic regulation of diacylglycerol kinase alpha promotes radiation-induced fibrosis.* Nat Commun, 2016. **7**: p. 10893.
6. Kuo, T.H., et al., *Matrix-Assisted Laser Desorption/Ionization Mass Spectrometry Typings of Edible Oils through Spectral Networking of Triacylglycerol Fingerprints.* ACS Omega, 2019. **4**(13): p. 15734-15741.
7. Tata, A., et al., *Detection of soft-refined oils in extra virgin olive oil using data fusion approaches for LC-MS, GC-IMS and FGC-Enose techniques: The winning synergy of GC-IMS and FGC-Enose.* Food Control, 2022. **133**.
8. La Nasa, J., F. Modugno, and I. Degano, *Liquid chromatography and mass spectrometry for the analysis of acylglycerols in art and archeology.* Mass Spectrom Rev, 2021. **40**(4): p. 381-407.
9. Pleik, S., et al., *Ambient-air ozonolysis of triglycerides in aged fingerprint residues.* Analyst, 2018. **143**(5): p. 1197-1209.
10. Tan, J.Y.B., et al., *Lipid Nanoparticle Technology for Delivering Biologically Active Fatty Acids and Monoglycerides.* Int J Mol Sci, 2021. **22**(18).
11. Nakmode, D., et al., *Fundamental Aspects of Lipid-Based Excipients in Lipid-Based Product Development.* Pharmaceutics, 2022. **14**(4).
12. Hou, X., et al., *Lipid nanoparticles for mRNA delivery.* Nat Rev Mater, 2021. **6**(12): p. 1078-1094.
13. Holcapek, M., G. Liebisch, and K. Ekroos, *Lipidomic Analysis.* Anal Chem, 2018. **90**(7): p. 4249-4257.

14. Gaudin, M., et al., *Atmospheric pressure photoionization as a powerful tool for large-scale lipidomic studies.* J Am Soc Mass Spectrom, 2012. **23**(5): p. 869-79.

15. Zhang, W., et al., *Deep-lipidotyping by mass spectrometry: recent technical advances and applications.* J Lipid Res, 2022. **63**(7): p. 100219.

16. Thomas, M.C., et al., *Ozone-Induced Dissociation: Elucidation of Double Bond Position within Mass-Selected Lipid Ions.* Analytical Chemistry, 2008. **80**(1): p. 303-311.

17. Ma, X. and Y. Xia, *Pinpointing double bonds in lipids by Paterno-Buchi reactions and mass spectrometry.* Angew Chem Int Ed Engl, 2014. **53**(10): p. 2592-6.

18. Zhang, W., et al., *Online photochemical derivatization enables comprehensive mass spectrometric analysis of unsaturated phospholipid isomers.* Nat Commun, 2019. **10**(1): p. 79.

19. Baba, T., et al., *Structural identification of triacylglycerol isomers using electron impact excitation of ions from organics (EIEIO).* J Lipid Res, 2016. **57**(11): p. 2015-2027.

20. Campbell, J.L. and T. Baba, *Near-complete structural characterization of phosphatidylcholines using electron impact excitation of ions from organics.* Anal Chem, 2015. **87**(11): p. 5837-45.

21. Ryan, E., et al., *Detailed Structural Characterization of Sphingolipids via 193 nm Ultraviolet Photodissociation and Ultra High Resolution Tandem Mass Spectrometry.* J Am Soc Mass Spectrom, 2017. **28**(7): p. 1406-1419.

22. Williams, P.E., et al., *Pinpointing Double Bond and sn-Positions in Glycerophospholipids via Hybrid 193 nm Ultraviolet Photodissociation (UVPD) Mass Spectrometry.* J Am Chem Soc, 2017. **139**(44): p. 15681-15690.

23. Cao, W., et al., *Large-scale lipid analysis with C=C location and sn-position isomer resolving power.* Nat Commun, 2020. **11**(1): p. 375.

24. Poad, B.L., et al., *High-Pressure Ozone-Induced Dissociation for Lipid Structure Elucidation on Fast Chromatographic Timescales.* Anal Chem, 2017. **89**(7): p. 4223-4229.

25. Calabrese, V., et al., *Electron-activated dissociation (EAD) for the complementary annotation of metabolites and lipids through data-dependent acquisition analysis and feature-based molecular networking, applied to the sentinel amphipod Gammarus fossarum.* Anal Bioanal Chem, 2024.

26. Myher, J.J., L. Marai, and A. Kuksis, *Identification of monoacyl- and monoalkylglycerols by gas–liquid chromatography–mass spectrometry using polar siloxane liquid phases.* Journal of Lipid Research, 1974. **15**(6): p. 586-592.

27. Wolrab, D., et al., *Ultrahigh-performance supercritical fluid chromatography / mass spectrometry in the lipidomic analysis*. TrAC Trends in Analytical Chemistry, 2022. **149**.

28. Cai, S.-S. and J.A. Syage, *Comparison of Atmospheric Pressure Photoionization, Atmospheric Pressure Chemical Ionization, and Electrospray Ionization Mass Spectrometry for Analysis of Lipids.* Analytical Chemistry, 2006. **78**(4): p. 1191-1199.

29. Abreu, S., et al., *Rapid assessment of triacylglycerol fatty acyls composition by LC-APPI(+)-HRMS using monoacylglycerol like fragments intensities.* Anal Chim Acta, 2021. **1178**: p. 338809.

30. Munoz-Garcia, A., et al., *Identification of complex mixtures of sphingolipids in the stratum corneum by reversed-phase high-performance liquid chromatography and atmospheric pressure photospray ionization mass spectrometry*. J Chromatogr A, 2006. **1133**(1-2): p. 58-68.

31. Robb, D.B. and M.W. Blades, *Effects of solvent flow, dopant flow, and lamp current on dopant-assisted atmospheric pressure photoionization (DA-APPI) for LC-MS. Ionizationvia proton transfer*. Journal of the American Society for Mass Spectrometry, 2005. **16**(8): p. 1275-1290.

32. Vaikkinen, A., T.J. Kauppila, and R. Kostiainen, *Charge Exchange Reaction in Dopant-Assisted Atmospheric Pressure Chemical Ionization and Atmospheric Pressure Photoionization*. J Am Soc Mass Spectrom, 2016. **27**(8): p. 1291-300.

33. Robb, D.B., D.R. Smith, and M.W. Blades, *Investigation of substituted-benzene dopants for charge exchange ionization of nonpolar compounds by atmospheric pressure photoionization.* J Am Soc Mass Spectrom, 2008. **19**(7): p. 955-63.

34. Mueller, P., R. Bonner, and G. Hopfgartner, *Controlled Formation of Protonated and Radical Cation Precursor Ions by Atmospheric Pressure Photoionization with muLC-MS Enables Electron Ionization and MS/MS Library Search.* Anal Chem, 2022. **94**(35): p. 12103-12110.

35. Riddell, N., et al., *Coupling supercritical fluid chromatography to positive ion atmospheric pressure ionization mass spectrometry: Ionization optimization of halogenated environmental contaminants.* International Journal of Mass Spectrometry, 2017. **421**: p. 156-163.

36. Herrera, L.C., M.A. Potvin, and J.E. Melanson, *Quantitative analysis of positional isomers of triacylglycerols via electrospray ionization tandem mass spectrometry of sodiated adducts.* Rapid Commun Mass Spectrom, 2010. **24**(18): p. 2745-52.

37. Christie, W.W., *Lipid analysis in oils and fats*. 2011, Springer: New York, NY. p. 97-98.